Research Article

Journal of Scientific Enquiry
Vol: 2 , Pages: 1-10

In-silico analysis via molecular docking study to identify the better potent inhibitor for the main protease (M^{pro}) of SARS-COV-2

Sourav Majumdar, Suvankar Karmakar, Anup Pramanik*

Department of Chemistry, Sidho-Kanho-Birsha University, Purulia – 723104, India

Received: 01.03.2022; accepted: 09.06.2022; published online: 30.06.2022

Abstract

In the end of the year 2019, a new strain of virus, named as COVID-19 was identified in the Wuhan city of China. As there are no specific treatment of drugs available in the market, people are searching for new drugs for combating COVID-19 disease. In our current research work, we have taken main protease (M^{pro}) as the receptor molecule (PDB ID 6LU7) and performed molecular docking study with various ligands like quercetin, chalcone, flavanone, hinokiflavone, isoflavone, robustaflavone, salannin, nafamostat and nimbosterol to understand the the mode of interaction which is helpful for designing new drugs for treating the virus. We have also done ADME (Absorption, Desorption, Metabolism and Excreation) property studies of the respective ligands. Our studies reveal that robustaflavone is the best potent inhibitors against the COVID-19 virus. However further researches are needed to investigate their potential medicinal use.

Keywords COVID-19, Main protease (M^{pro}), Molecular Docking, ADME properties

1. Introduction

In the end of the year 2019, a new medical emergency appeared worldwide due to the rapid outbreak of SARS-COV-2 (namely COVID-19) which was very much unprecinented. Several attempts have been made worldwide to get rid of the infectious virus by clinically but a few of them became successful [1-13]. However, in recent years, novel computational approaches have been done to design and utilize several potential drug candidates against various diseases. Molecular Docking and pharmacophore analysis are the two main approaches in drug discovery process [2,3]. Since there are no current therapeutics to treat COVID-19, drug repositionning is the only way to get rid of it. However, there are several drug compounds which are available in the market for the COVID-19 main protease (M^{pro}) [4,5]. In order to identify the best drug repositionning strategy to treat COVID-19 disease, many clinical trials have also been done so far. Some clinical trials propose that anti-HIV, antimalarial drugs have a great therapeutic effect against the COVID-19 disease [6-8]. With the help of sequence analysis process, it can be said that SARS-COV-2 belongs to two groups i.e. SARS-COV and MARS-COV and the present SARS-COV-2 belongs to the beta genome [9-12]. In case of drug discovery process the crucial step is the interaction of the target protein with the ligand in order to estimate their pharmocological properties. Molecular docking, molecular dynamics simulations, drug likeliness and in-silico analyses have been done to know the respective pharmacological properties and binding affinities of the ligands with the respective protein [14-16]. Explorations of some compounds with medicinal activity have also been carried out to find their suitable acivity against the different proteins of SARS-COV-2 [17-19]. In this particular work, we have choosen M^{pro} i.e. main protease of SARS-COV-2 as the target protein (Protein Data Bank (PDB) ID 6LU7) and different ligand moieties i.e. quercetin, chalcone, flavanone, hinokiflavone, isoflavone, robustaflavone, salannin, nafamostat and nimbosterol to dock them in order to understand the drug-protein interactions. Among these drugs the highest docking score i.e., the highest binding energy (-8.17 kcal/mol) is found for 6LU7-robustaflavone complex. The interactions of the drug molecules with the protein, 6LU7 have also been analysed using protein-ligand interaction profiler (PLIP) and finally, Swiss ADME server is used for the calculation of pharmacological properties. Figure 1 represents the structures of the nine ligands Quercetin, Chalcone, Flavanone, Hinokiflavone, Isoflavone, Robustaflavone, Salannin, Nafamostat and Nimbosterol.

[1] Email: anup.pramanik@sbku.ac.in

 DOI: https://doi.org/10.54280/jse.222101

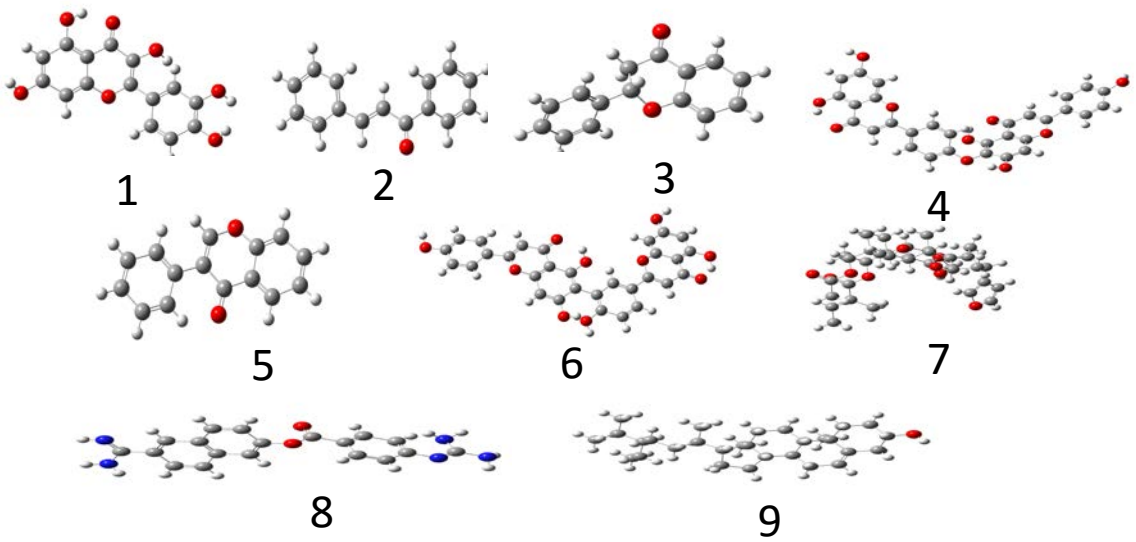

Fig. 1. 3D Structures of 1. Quercetin 2. Chalcone 3. Flavanone 4. Hinokiflavone 5. Isoflavone 6. Robustaflavone 7. Salannin 8. Nafamostat 9. Nimbosterol drew with the help of Gaussview software.

2. Methodology

2.1 Protein preparation for docking

In this particular study, at first, we obtain a protein moeity from the RCSB protein data bank (PDB ID 6LU7) [20]. Then with the help of Molecular Graphics Laboratory Tools (MGL Tools) and AutoDock tools [21], the protein is selected first in PDB format. After that, by deleting water and other heteroatoms from the protein moeity, followed by subsequent adding of polar hydrogens and Kolmann charges the protein gets saved into PDBQT (Protein Data Bank with partial charge and active torsons) format in order to prepare it for docking. With the help of python molecular viewer [22], the crystal structure of the 6LU7 protein is obtained and enlisted below. Noteworthy, the chain A of the receptor molecule is used for docking and as the chain C is the inhibitor part of the molecule, it has been omitted. Here the crystal structure of the main protease of SARS-COV-2 has been represented in Figure 2. *2.2 Ligand preparation for docking*

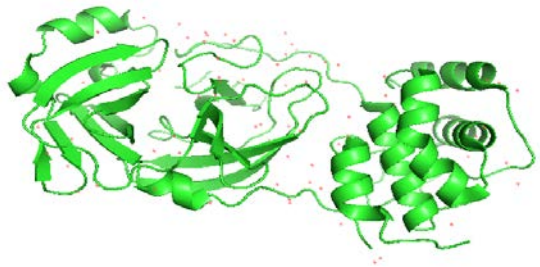

Fig. 2. The crystal structure of COVID-19 $3CL^{Pro}$ (PDB ID 6LU7).

First of all, nine ligands were downloaded from PubChem online liberty in SDF format. The ligands were then converted to PDB format with the help of python molecule viewer software and then, with the help of AutoDock tools, the ligands were saved in PDBQT format in order to prepare it for docking.

2.3 Molecular docking study

After preparation of both protein and the ligands, both the receptor protein molecule (PDB ID 6LU7) and the ligands are enclosed in a grid box and the grid box dimensions were set as 100×100×100 $Å^3$ with the grid spacing value of 1 Å and the central co-ordinates of the grid were positioned as -26.283, 12.599 and 58.966. The present ligand docking calculations were done by employing Lamarckian GA (Genetic Algorithm) and the other default parameters as implemented in AutodockVina. After the docking gets finished the output files were analyzed by using python molecular viewer software. The different docking scores of ligands have been shown below in Table 1.

Table 1. Docking scores of different ligands (Lowest binding energy) with the $3CL^{Pro}$ of SARS-COV-2.

Sl. No.	Entry Name (ligand)	Docking Score (kcal/mol)	PubChem CID
1	Quercetin	-5.28	5280343
2	Chalcone	-5.76	637760
3	Flavanone	-6.54	10251
4	Hinokiflavone	-5.93	5281627
5	Isoflavone	-6.13	72304
6	Robustaflavone	-8.17	5281694
7	Salannin	-8.03	6437066
8	Nafamostat	-5.91	4413
9	Nimbosterol	-6.28	222284

3. Ligand properties

In our work we have listed molecular weight and several uses of the 9 ligands in Table 2.

Table 2. Molecular weight and uses of different ligands

Serial No	Ligand name	Molecular weight (g/mol)	Uses of the ligand
1	Quercetin	302.23	Anti-oxidant, Anti-inflammatory
2	Chalcone	208.25	Anti-inflammatory, Anti-tumor
3	Flavanone	224.25	Anti-inflammatory, Anti-fungal, Anti-microbial
4	Hinokiflavone	538.46	Neuroprotective agent, Anti-neoplastic agent
5	Isoflavone	222.24	Anti-oxidant, Anti-cancer
6	Robustaflavone	538.5	Anti-oxidant, Anti-neoplastic, Anti-viral and Anti-microbial
7	Salannin	596.71	Anti-feedant
8	Nafamostat	347.4	Anti-viral, Anti-inflammatory
9	Nimbosterol	414.7	Anti-inflammatory, Anti-fungal

4. Method of calculation of docking score

Mainly molecular docking in between a protein and ligand occurs via the lock and key mechanism. In order to predict the strength of the molecular docking, a term scoring function is used. In the case of AutoDock Vina, different algorithms are used in order to find the lowest binding energy conformation. In scoring function (C), both intermolecular (C_{inter}) and intramolecular (C_{intra}) terms are used and it is represented as

$$C = C_{inter} + C_{intra}$$

Finally, in order to validate the docking protocol, RMSD between the protein-ligand complex gets checked, which should be < 2 Å. In our work, we have checked that RMSD value of all protein-ligand complex as < 2 Å, where Lamarckian GA is used to find out better lowest energy conformation [23].

5. Result and Discussion

From the molecular docking studies of the 9 ligands i.e. Quercetin, Chalcone, Flavanone, Hinokiflavone, Isoflavone, Robustaflavone, Salannin, Nafamostat, Nimbosterol with the $3CL^{Pro}$ (3-Chymotrypsin like protease) of SARS-COV-2 (PDB ID 6LU7), it is observed that Robustaflavone has the highest docking score (docking energy -8.17 kcal/mol) with the $3CL^{Pro}$ of SARS-COV-2. Here, the binding residues of the 6lu7-robustaflavone and the other complexes are visualized using protein ligand

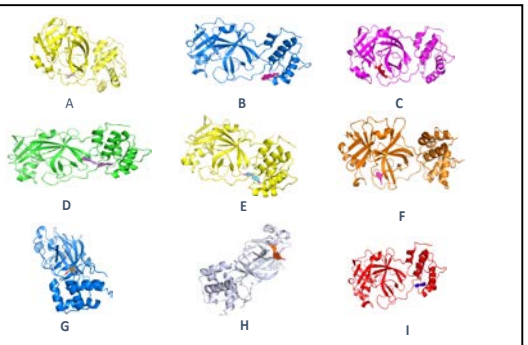

Fig. 3. Protein-ligand docked crystal structures of A) 6LU7-Chalcone B) 6LU7-Nimbosterol C) 6LU7-Salannin D) 6LU7-Hinokiflavone E) 6LU7-Nefamostat F) 6LU7-Flavanone G) 6LU7-Isoflavone H) 6LU7-Robustaflavone I) 6LU7-Quercetin complexes visualised using python molecular viewer software.

interaction profiler (PLIP) software and also with the help of LIGPLOT+ software. With the help of AutoDock Tools the remaining docking energies of Quercetin, Chalcone, Salannin, Nafamostat, Nimbosterol, Hinokiflavone, Isoflavone and Flavanone were found to be -5.28, -5.76,-8.03,-5.91,-6.28,-5.93,-6.13 and -6.54 kcal/mol, respectively. The different protein-ligand docked crystal structures are given below in Fig. 3. From the Protein-ligand interaction (Fig. 4) profiler software image it is clear that $3CL^{Pro}$ of SARS-COV-2 interacts with quercetin mostly via the amino acid residue HIS 41, MET165, GLN189 and it forms hydrogen bonds with TYR54, HIS164, GLU166, ASP187, THR190 and GLN192. The corresponding length of bonds and other properties are enlisted in Table 3.

Table 3. Different interactions and distances (in Å) between the amino acid residues of the receptor and the ligand molecule (quercetin).

Hydrophobic Interactions

Sl. No.	*Residue*	*Amino acid*	*Distance (Å)*	*Ligand*
1	41	HIS	3.74	6
2	165	MET	3.78	2
3	189	GLN	3.62	4

Hydrogen bonds

Serial No.	Residue	Amino Acid	Distance H-A	Distance D-A
1	54	TYR	2.31	2.80
2	164	HIS	3.25	3.57
3	166	GLU	2.59	3.60
4	187	ASP	2.00	2.96
5	190	THR	2.29	2.87
6	192	GLN	2.39	2.85
7	192	GLN	2.54	3.52

Pi-stacking

Index	Residue	Amino acid	Distance
1	41	HIS	4.58

 DOI: https://doi.org/10.54280/jse.222101

Fig. 4. Different binding modes of 6LU7-Quercetin complex visualised using protein-ligand interaction profiler (PLIP) software.

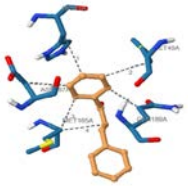

Fig. 5. Different binding modes of 6LU7-Chalcone complex visualized using protein-ligand interaction profiler (PLIP) software.

Fig. 5 demonstrates that $3CL^{Pro}$ of SARS-COV-2 interacts with chalcone mostly via the amino acid residues HIS41, MET49, MET165, ASP187 and GLN189 and these bonds are non-covalent bonds. Table 4 provides the corresponding bond lengths and the other properties.

Table 4. Different interactions and distances (in Å) between the amino acid residues of the receptor and the ligand molecule (chalcone).

Index	Residue	Amino acid	Distance (Å)	Ligand atom
1	41	HIS	3.74	6
2	49	MET	3.94	5
3	165	MET	3.38	8
4	165	MET	3.33	9
5	187	ASP	3.81	7
6	189	GLN	3.27	4

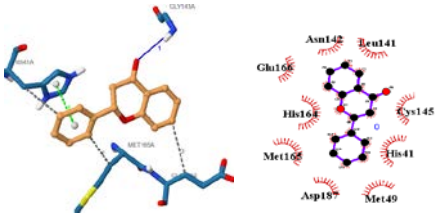

Fig. 6. Different binding modes of 6LU7-Flavanone complex visualised using PLIP and LIGPLOT+ software.

From this protein-ligand interaction profile (Fig. 6), it is clear that $3CL^{Pro}$ of SARS-COV-2 interacts with the ligand flavanone mostly via the amino acid residues HIS41, MET165, GLU166 and it forms H bonds with the amino acid residues GLY143. The corresponding length of bonds and other properties are enlisted in Table 5.

Table 5. Different interactions and distances (in Å) between the amino acid residue of the receptor and the ligand (Flavanone).

Hydrophobic interactions

Index	Residue	Amino acid	Distance	Ligand atom
1	41	HIS	3.69	14
2	165	MET	3.55	17
3	166	GLU	3.98	6

Hydrogen bonds

Index	Residue	Amino acid	Distance H-A	Distance D-A
1	143	GLY	2.76	3.77

Pi Stacking

Index	Residue	Amino acid	Distance
1	41	HIS	4.00

As shown in Table 6, hinokiflavone mostly interacts via the amino acid residues THR25, GLN189 and it forms H bonds with the amino acid residues THR26 and GLU166. The corresponding interaction profile is shown in Figure S1.

Table 6. Different interactions and distances (in Å) between the amino acid residue of the receptor and the ligand (Hinokiflavone).

Hydrophobic interactions

Index	Residue	Amino acid	Distance	Ligand atom
1	25	THR	3.24	42
2	189	GLN	3.82	20

Hydrogen bonds

Index	Residue	Amino acid	Distance H-A	Distance D-A
1	26	THR	1.87	2.84
2	26	THR	2.07	2.73
3	166	GLU	2.32	3.25

In case of isoflavone, it mostly involves H-bonding interactions via LYS12, LYS97 and PRO99 amino acid residues with $3CL^{Pro}$ of SARS-COV-2 as demonstrated in Figure S2 and the corresponding bond lengths are shown in Table 7.

Table 7. Different interactions and distances (in Å) between the amino acid residue of the receptor and the ligand (Isoflavone).

Hydrophobic interactions

Index	Residues	Amino acid	Distance	Ligand atom
1	12	LYS	3.85	13
2	97	LYS	3.50	16
3	99	PRO	3.87	4

From this protein-ligand interaction (Fig. 7) profiler image and LIGPLOT+ image it is clear that $3CL^{Pro}$ of SARS-COV-2 interacts with the ligand robustaflavone mostly via the amino acid residues THR25 and it forms hydrogen bonds with THR25, THR26, ASN42, GLN189 and THR190. The corresponding H-bonding distances and other interaction parameters are enlisted in Table 8.

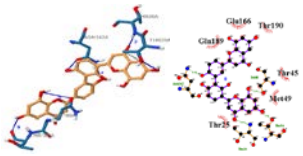

Fig. 7. Different binding modes of 6LU7-Robustaflavone complex visualised using PLIP and LIGPLOT+ software.

Table 8. Different interactions and distances between the amino acid residue of the receptor and the ligand (Robustaflavone).

Hydrophobic Interaction

Index	Residue	Amino acid	Distance	Ligand atom
1	25	THR	3.62	36

Hydrogen bonds

Index	Residue	Amino Acid	Distance H-A	Distance D-A
1	25	THR	2.20	2.88
2	26	THR	2.06	3.06
3	142	ASN	2.26	3.06
4	142	ASN	2.44	3.10
5	189	GLN	3.13	3.77
6	190	THR	2.42	2.90

The ligand salannin mostly interacts with the $3CL^{Pro}$ of SARS-COV-2 via the amino acid residues MET165, GLN189 and it forms salt bridges with HIS41residue as shown in Figure S3. The corresponding bond lengths and other interaction parameters are enlisted in Table 9.

Table 9. Different interactions and distances (in Å) between the amino acid residue of the receptor and the ligand (Salannin).

Hydrophobic interactions

Index	Residue	Amino acid	Distance	Ligand atom
1	165	MET	3.87	7
2	189	GLN	3.67	7

Salt bridges

Index	Residue	Amino acid	Distance
1	41	HIS	3.91

As demonstrated in Figure S4, $3CL^{Pro}$ of SARS-COV-2 interacts with the ligand nafamostat mostly via the amino acid residue MET165, GLN189 and it forms hydrogen bonds with the residues THR26, GLY143 and THR190. The corresponding bond lengths and other interaction parameters are given in Table 10

Table 10. Different interactions and distances (in Å) between the amino acid residue of the receptor and the ligand (Nafamostat)

Hydrophobic interactions

Index	Residue	Amino acid	Distance	Ligand
1	165	MET	3.31	8
2	189	GLN	3.80	1

Hydrogen Bonds

Index	Residue	Amino Acid	Distance H-A	Distance D-A
1	26	THR	2.25	2.76
2	143	GLY	2.64	3.44
3	190	THR	2.30	2.92

We present the protein – ligand interaction profile for 6LU7 and nimbosterol in Figure S5 and from the figure it is clear that $3CL^{Pro}$ of SARS-COV-2 interacts with the ligand nimbosterol mostly via the amino acid residues HIS41, GLY143, CYS145, HIS163,HIS164, MET165, GLU166, PRO168 and GLN189. Table 11 enlists the corresponding bond lengths and other interaction parameters.

Table 11. Different interaction and distances (in Å) between the amino acid residue of the receptor and the ligand (Nimbosterol)

Hydrophobic interactions

Index	Residue	Amino acid	Distance	Ligand atom
1	41	HIS	3.92	5806
2	143	GLY	3.70	5807
3	145	CYS	3.49	5807
4	163	HIS	3.92	5801
5	164	HIS	3.95	5801
6	165	MET	3.45	5796
7	166	GLU	3.33	5791
8	168	PRO	3.53	5781
9	189	GLN	3.73	5788

Finally, drug likeliness of the studied ligands are presented in Table 12 which basically accounts five parameters as demonstrated in the table. Here, in this table since all ligands follow Lipinski's rule of five (Ro5) i.e. MW < 500g/mol, No of H bond donors ≤ 5, number of H bond acceptors ≤ 10, MLOGP < 5, hence we can say that all the ligands are orally administrable candidates as drug.

Table 12. ADME Properties of selected SARS-COV-2 inhibitors with the help of SWISSADME prediction (http://www.swissadme.ch/)

Ligand/Drug	ADME properties	Drug likeliness
Quercetin	Molecular weight 302.24 g/mol	YES

	No of H bond donors 5 No of H bond acceptors 7 Molar refractivity 78.04 Violation no	
Chalcone	Molecular weight 208.26 g/mol No of H bond donors 0 No of H bond acceptors 1 Molar refractivity 66.25 Violation no	YES
Nafamostat	Molecular weight 347.37 g/mol No of H bond donor 4 No of H bond acceptor 4 Molar refractivity 101.24 Violation no	YES
Robustaflavone	Molecular weight 538.46 g/mol No of H bond donor 5 No of H bond acceptor 10 Molar refractivity 146.97 Violations 1 MW>500 g/mol	YES
Hinokiflavone	Molecular weight 538.46 g/mol No of H bond donors 5	YES
	No of H bond acceptors 10 Molar refractivity 146.03 Violation 1 MW>500 g/mol	
Flavanone	Molecular weight 224.25 g/mol No of H bond donors 0 No of H bond acceptors 2 Molar refractivity 65.50 Violation no	YES
Isoflavone	Molecular weight 222.24 g/mol No of H bond donors 0 No of H bond acceptors 2 Molar refractivity 67.92 Violation no	YES
Salannin	Molecular weight 596.71 g/mol No of H bond donors 0 No of H bond acceptors 9 Molar refractivity 156.80 Violation 1 MW>500	YES
Nimbosterol	Molecular weight 414.71 g/mol No of H bond donors 1 No of H bond acceptors 1	YES

	Molar refractivity 133.25 Violation 1 MLOGP>4.15	

6. Conclusion

Since the outbreak of the COVID 19 pandemic, it becomes a global healthcare problem to each and everybody and for this reason the economic loss remain unbeaten. No specific medicines are available till now. In this particular study we have taken 9 compounds for molecular docking and in silico analysis to find the best potent inhibitor for SARS-COV-2 of $3CL^{Pro}$ and robustaflavone is found to have the highest docking score among these compounds. Hence, from the above theoretical studies it can be inferred that the compound robustaflavone can act as a potent inhibitor against the COVID-19 main protease (M^{pro}) and thus we can say that it can show various antiviral and antimicrobial activity in case of the COVID-19 disease.

References

1) M Hastantram, S Ramaiah, R Vishwakarma and U R Shannker, Molecular docking analysis of selected natural products from plants for inhibition of SARS-COV-2 main protease , Current Science, 118, 7 (2020).

2) R R Narkhede, R S Cheke, J P Ambhore and S D Shinde, The Molecular Docking Study of Potential Drug Candidates Showing Anti COVID 19 Activity by Exploring of Therapeutic Targets of SARS-COV-2, Ejmo, 4(3), 185-195 (2020).

3) S Beura and C Prabhakar, In Silico Strategies for Probing chloroquine based inhibitors against SARS-COV-2, Journal of Biomolecular Structure and Dynamics, 39, 3747-3759 (2020).

4) S Chtita, A Belhassam, A Aouidate, S Belaidi, M Bouachrine and T Lakhlifi, Discovery of potent SARS-COV-2 inhibitors from approved antiviral drugs via docking and virtual screening, Combinatorial Chemistry and High Throughput Screening, 24(3), 441-454 (2021).

5) S V Stoddard, S D Stoddard, B K Oelkers, K Fitts, K Whalum, K X Whalum, A D Hemphill, J Manikonda, L M Martinez, E G Riley, C M Roof, N Sarwar, D M Thomas, E Ulmer, F E Wallace , P Pandey and S Roy , Optimization Rules for SARS-COV-2 M^{pro} Antivirals: Ensemble Docking and exploration of the coronavirus protease active site, Viruses, 12(9), 942 (2020).

6) E Mamidala, R Davella , S Gurappu and P Shivakrisna , In silico Identification of clinically approved medicines against the main protease of SARS-COV-2, causative agent of COVID 19, Arxiv, 2004, 12055 (2020).

7) A Ubani, F Agwom, O Ruthmorenikeji, S Nathan , P Luka, A Umera, U RR, S Omale, N E Nnadi and J C Aguiyi, Molecular Docking Analysis of some phytochemicals on two SARS-COV-2 targets potential lead compounds against two target sites of SARS-COV-2 obtained from plants, BioRxiv (2020) doi: https://doi.org/10.1101/2020.03.31.017657.

8) A K Peele, C P Durthi, T Srihansa, S Krupanidhi,V A Sai ,J D Babu, M Indira, R A Reddy and T C Venkateswarulu , Molecular Docking and Dynamic simulations for antiviral compounds against SARS-COV-2: A computational study, Informatics in medicine unlocked, 19, 100345 (2020).

9) S L Khan, F A Siddhiqui, S P Jain and G M Sonwane, Discovery of potential inhibitors of SARS-COV-2 (COVID 19) main protease (M^{pro}) from Nigella Sativa (Black Seed) by molecular docking study, Bentham Science, 2(3), 384-402 (2021).

10) S Mondal, A Karmakar, T Mallick and N A Begum, Exploring the efficacy of naturally occurring biflavone based antioxidants towards the inhibition of the SARS-COV-2 spike glycoprotein mediated membrane fusion, Virology, 556, 133-139 (2021).

11) A Agrawal, N K Jain, N Kumar and G T Kulkarni, Molecular Docking study to identify potential inhibitor of COVID 19 main protease enzyme: an in silico approach, Chemrxiv (2020) 10.26434/chemrxiv.12170904.v1.

12) S Khaerunnisa, H Kurniawan , R Awaluddin, S Suhartati and S Soetjipto, Potential Inhibitor of COVID 19 Main protease (M^{pro}) from several medicinal plant compounds by molecular docking study, Preprint (2020), doi: 10.20944/preprints202003.0226.v1.

13) M I Choudhary, M Shaikh, A T Wahab and A U Rahman, In silico identification of potential inhibitors of key SARS-COV-2 3CL hydrolase (MPro) via molecular docking, MMGBSA predictive binding energy calculations and molecular dynamics simulations, Plos One, 15(7), e0235030 (2020)

14) P Chowdhury , In silico investigation of phytoconstituents from Indian medicinal herb 'TinosphoraCordipholia (giloy)' against SARS-COV-2 (COVID 19) by molecular dynamics approach, Journal of Biomolecular Structure and Dynamics, 39(17), 6792-6809 (2021).

15) P Rao, A Shukla, P Parmar, R M Rawal, B Patel, M Saraf and D Goswami, Reckoning a fungal metabolite ,Pyranonigrin A as a potential main protease (M^{pro}) inhibitor of novel SARS-COV-2 virus identified using docking and molecular dynamics simulation , Biophysical Chemistry, 164, 106425 (2020).

16) G Zhou, L Stewart ,G Reggiano and F Dimaio, Computational drug repurposing studies on SARS-COV-2 protein targets, Chemrxiv (2020) 10.26434/chemrxiv.12315437.v1.

17) M R F Pratama, H Poerwono and S Siswodihardjo, Molecular docking of novel 5-O-benzoylpinostrobin derivatives as SARS-COV-2 main protease inhibitors, Pharmaceutical Sciences, 26(1), 63-77 (2020).

18) S Adem, V Eyupoglu, I Sarfraz , A Rasul and M Ali, Identification of potent COVID 19 main protease (M^{pro}) inhibitors from natural polyphenols: An in silico strategy unveils a hope against CORONA, Preprints (2020) doi: 10.20944/preprints202003.0333.v1.

19) A Ghaleb, A Aouidate, H B E Ayouchia, M Aarjane, H Anane and S E Stiriba, In silico molecular investigations of pyridine -N-Oxide compounds as potential inhibitors of SARS-COV-2: 3D-QSAR, molecular docking modelling and ADMET screening, Journal of Biomolecular Structure and Dynamics, 39, 6339-6851 (2020).

20) P W Rose, A Prlic, A Altunkaya, C Bi, A R Bradly, C H Christie, L D Costanzo, J M Duarte, S Dutta, Z Feng, R K Green, D S Goodsell, B Hudson, T Karlo, R Lowe, E Peisach, C Randle, A S Rose, C Shao, Y P Tao, Y Valasatava, M Voigt, J D Westbrook, J Woo, H Yang, J Y Young, C Zardecki, H M Berman, S K Burley, The RCSB protein data bank: integrative view of protein, gene and 3D structural information, Nucleic Acids Research,45(D1), D271–D281(2016).

21) A Rudnitskaya, B Torok, M Torok, Molecular Docking of enzyme inhibitors, Biochemistry and Molecular Biology Education,38(4), 261-265(2010).

22) S Yuan, H C S Chan, Z. Hu, Using PyMOL as a platform for computational drug design, Wiley Interdisciplinary Reviews: Computational Molecular science, 7(2), e1298(2017).

23) O Trott, A J Olson, Software News and Update AutoDock Vina: Improving the Speed and Accuracy of Docking with a New Scoring Function, Efficient Optimization, and Multithreading, Journal of Computational Chemistry, 31(2), 455-461 (2010).